IOP Publishing Superconductor Science and Technology
Supercond. Sci. Technol. 33 (2020) 055007 (6pp) https://doi.org/10.1088/1361-6668/ab7d8f

Superconductivity in single crystalline $LuPd_2Si_2$ probed by heat capacity measurements

G Chajewski, P Wiśniewski, D Gnida, A P Pikul and D Kaczorowski

Institute of Low Temperature and Structure Research, Polish Academy of Sciences, P Nr 1410, 50-590 Wrocław 2, Poland

E-mail: G.Chajewski@intibs.pl

Received 17 December 2019, revised 19 February 2020
Accepted for publication 6 March 2020
Published 30 March 2020

Abstract

Single-crystalline samples of $LuPd_2Si_2$ were studied by means of low-temperature specific heat measurements performed in a magnetic field oriented along two main crystallographic directions. The compound was found to be superconducting below 0.6 K, in agreement with previous reports. Detailed analysis of the phase-transition anomaly revealed that $LuPd_2Si_2$ is a BCS-like superconductor with anisotropic properties and a possible two-gap character.

Keywords: $LuPd_2Si_2$, single crystal growth, heat capacity, superconductivity

(Some figures may appear in colour only in the online journal)

1. Introduction

Binary and ternary intermetallic compounds have been of unwavering interest to the scientific community for several decades and studies of their physical properties constitute a significant part of modern solid state physics. One of the most numerous and most intensively studied materials are f-electron systems with the stoichiometry 1:2:2, which have been thoroughly investigated due to their electronic structure which gives rise to a great variety of magnetism-related physical phenomena (see e.g. [1]). Another group of widely-investigated 1:2:2 compounds are iron arsenides, being a surprising example of the coexistence of magnetism and superconductivity [2, 3].

Motivated by those discoveries, we have recently performed a systematic re-investigation of non-magnetic 1:2:2 silicides and germanides, which have resulted in several reports on properties of the whole series of compounds [4–8], as well as more detailed studies of selected superconductors both on polycrystalline samples [9, 10] and single crystals [11, 12], confirming or discovering the presence of superconductivity in several compounds.

Among the silicides investigated, $LuPd_2Si_2$ has been only briefly characterized, although it has been known as a superconductor for more than 30 years. In the first report [13], the crystal structure and temperature-dependent magnetic susceptibility of the compound were described and only very recently, some electrical transport and heat capacity data obtained on polycrystalline samples was published [14]. The results indicated the onset of superconductivity at a T_c of about 0.6 K.

Here, we present a detailed description of the superconducting state in single-crystalline $LuPd_2Si_2$ derived from low-temperature specific heat experiments performed down to 50 mK.

2. Materials and methods

Single crystals of $LuPd_2Si_2$ were synthesized using a PdSi binary flux method used previously to grow YPd_2Si_2 crystals [12]. The high purity constituent elements were initially melted in an electric arc in the molar ratio Lu:Pd:Si of 1:4:4 (in the first step, Pd was melted together with Si, lutetium was added afterwards). The crumbled material was placed in an alumina crucible and sealed together with another inverted crucible covered with a molybdenum foil strainer inside a fused silica tube under partial argon atmosphere. In order to

avoid problems associated with the silica softening at high temperatures, the pressure of argon was adjusted to be close to atmospheric pressure at 1200°C. The ampoule was heated up to 1200°C, kept at this temperature for 48 h in order to achieve proper homogenization of the batch and then slowly cooled down to 1100°C. The excess flux was subsequently removed using a centrifuge.

The crystal structure of the obtained single crystals was examined on powdered crystals by means of x-ray diffraction using an X'pert Pro PANalytical powder diffractometer with Cu K_α radiation. The Rietveld method implemented into the Fullprof software [15] was used to analyze the collected data. The quality and orientation of crystals were checked by means of Laue x-ray backscattering using a PROTO Manufacturing LAUE single crystal orientation system. The chemical composition of the obtained single crystals was examined by energy dispersive spectroscopy (EDS) on a FEI scanning electron microscope (SEM) equipped with an EDAX Genesis XM4 spectrometer. The spectra were measured at several individual spots and the collected data were averaged. Specific heat measurements were performed in the range from 50 mK up to room temperature using a standard time-relaxation method [16] implemented in a commercial Quantum Design PPMS platform equipped with a ^{3}He cryostat and a ^{3}He–^{4}He dilution refrigerator. Zero field measurements in ^{3}He regime (down to 0.35 K) were performed on three different crystals. Since the results were found to be reproducible, one of the crystals was chosen for measurements at lower temperatures and in magnetic fields. Before the low-field experiments, we performed zeroing of the magnetic field using a dedicated sequence with a field strength approaching a zero value in an oscillating manner, resulting in a remanent field of about 0.1 mT.

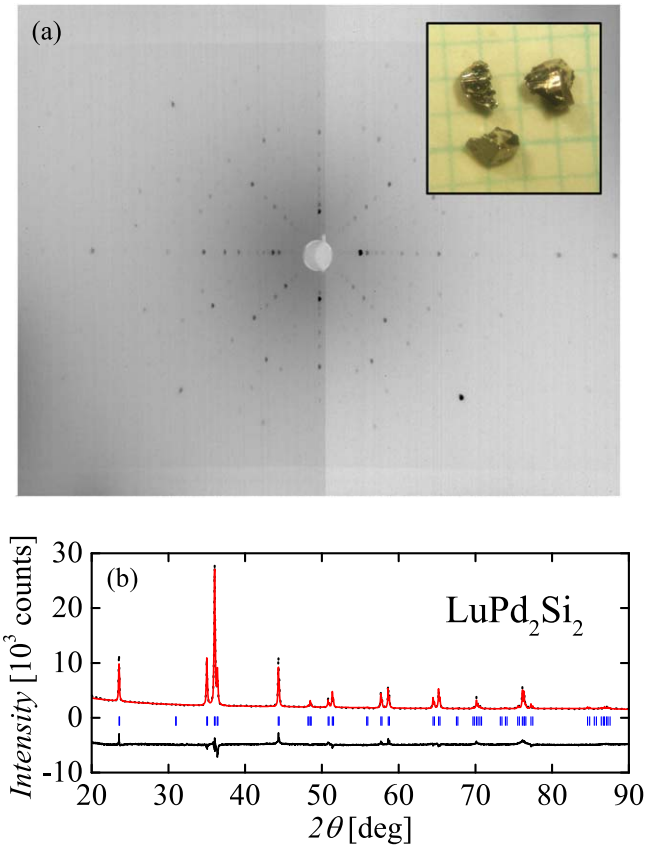

Figure 1. (a) x-ray Laue back-scattering image of $LuPd_2Si_2$ single crystal; inset: a photograph of single crystals on a millimeter grid. (b) x-ray powder diffraction pattern (black dots) of $LuPd_2Si_2$, calculated profile (red solid curve) and a difference plot (black solid line below). Vertical ticks indicate the refined positions of Bragg reflections.

3. Results and discussion

3.1. Crystal structure and elemental composition

Figure 1(a) displays the Laue back-reflection photography obtained on a selected $LuPd_2Si_2$ single crystal. A clear diffraction pattern with sharp spots indicates the high quality of the crystal and manifests four-fold rotational symmetry around the *c*-axis. By rotating the single crystal and performing several measurements at different spots we obtained consistent Laue diffraction images, which suggests that the sample is single grain. The analysis of the collected x-ray powder diffraction pattern (see figure 1(b)) confirmed the tetragonal $ThCr_2Si_2$-type crystal structure of the studied compound and proved the single-phase character of the specimens studied. While the refined lattice parameters $a = 4.0838(3)$ Å and $c = 9.8729(2)$ Å are consistent with the previously reported ones [8, 13, 14], the derived atomic coordinate $z_{Si} = 0.3802(5)$ differs slightly from that obtained for the polycrystalline sample (0.3866(11)) [8]. Moreover, the crystals were found to be homogeneous, with the experimentally determined composition of Lu/Pd/Si = 19.9/38.9/41.2 at.% being very close to the expected stoichiometry.

3.2. Specific heat

The normal-state specific heat of $LuPd_2Si_2$ measured in zero magnetic field and at temperatures up to 300 K (not shown here) was found to be consistent with the previously reported data [14]. In particular, the parameters describing electron and phonon (Debye and Einstein) contributions in the polycrystalline sample allow to reproduce well the temperature variation of the specific heat of our single crystalline specimen. Therefore, our further analysis was focused on the low-temperature range covering the superconducting phase transition.

Figure 2 shows the temperature dependence of the specific heat C_P (T) of $LuPd_2Si_2$ for two different orientations of applied magnetic field relative to crystal axes. A large and sharp λ-shaped anomaly visible on the zero-field curve manifests bulk superconducting phase transition with $T_c = 0.60$ K. Applying magnetic field of about 25 mT for $H \parallel c$ and 12 mT for $H \perp c$ moves the peak of C_P (T) below the temperature range covered in our study.

The $C_P(T)$ curve measured in the normal state (i.e. in $\mu_0 H = 25$ mT, which was sufficient to suppress the superconductivity for both directions of applied field) was used to estimate the Sommerfeld coefficient γ_n and the phononic

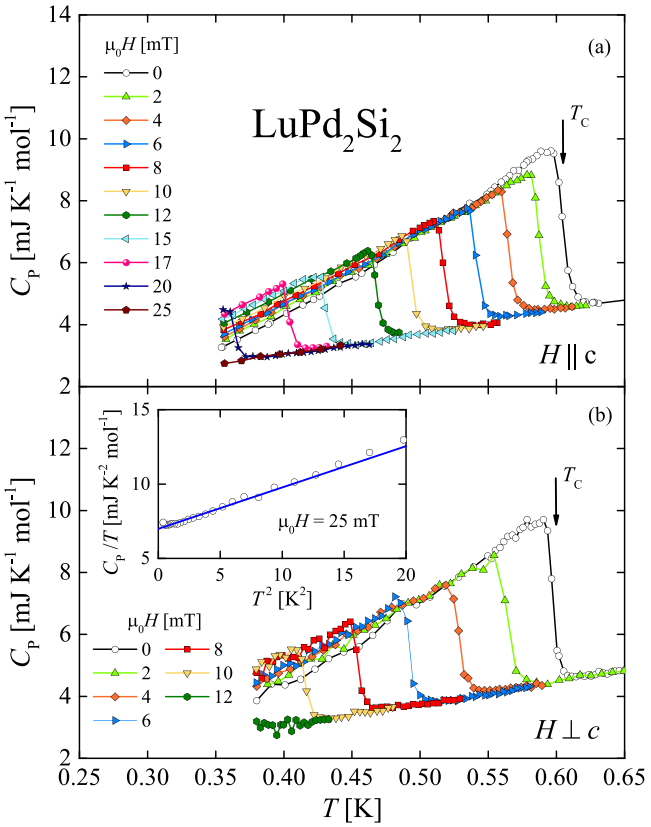

Figure 2. Low-temperature specific heat of single-crystalline $LuPd_2Si_2$ measured in various magnetic fields applied (a) parallel and (b) perpendicular to the *c*-axis; T_c marks the superconducting transition temperature. Inset: normal-state specific heat (measured in 25 mT); solid line is a fit of equation (1) to the experimental data.

specific heat coefficient β from the Debye approximation:

$$C_P(T) = \gamma_n T + \beta T^3. \quad (1)$$

The least-squares fitting procedure (see the solid line in the inset to figure 2(b)) yielded the parameters $\gamma_n = 7.0\ \mathrm{mJK^{-2}\,mol^{-1}}$ and $\beta = 0.28\ \mathrm{mJK^{-4}mol^{-1}}$. The latter value is related to the Debye temperature Θ_D via the expression $\beta = (12/5)\pi^4 nR/\Theta_D^3$, where n is the number of atoms per formula unit and R is the universal gas constant. In this way we found that Θ_D in $LuPd_2Si_2$ is of about 327 K, which is similar to the values of Θ_D obtained for polycrystalline samples of isostructural LuT_2Si_2 systems [8].

The so-derived Debye temperature may be further used to estimate the electron–phonon coupling constant λ_{el-ph} from the inverted McMillan's relation [17]:

$$\lambda_{el-ph} = \frac{1.04 + \mu^* \ln(\Theta_D/1.45T_c)}{(1 - 0.62\mu^*)\ln(\Theta_D/1.45T_c) - 1.04}. \quad (2)$$

Taking the Coulomb pseudopotential constant $\mu^* = 0.13$ one gets $\lambda_{el\text{-}ph} = 0.41$, which suggests realization of the weak-coupling superconductivity scenario in $LuPd_2Si_2$. Then, from the formula $N_b(E_F) = 3\gamma_n/[\pi^2 k_B^2(1 + \lambda_{el-ph})]$ one can calculate the bare density of states at the Fermi level to be here $N_b(E_F) = 2.1\ \mathrm{eV^{-1}f.u.^{-1}}$

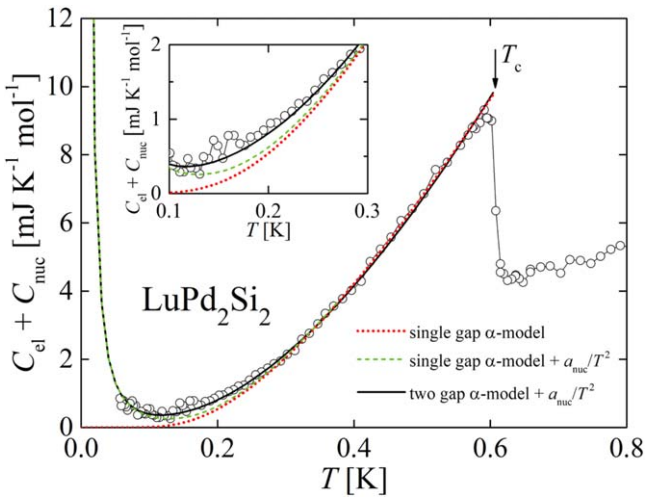

Figure 3. Low-temperature non-phononic specific heat of single-crystalline $LuPd_2Si_2$ measured in zero magnetic field; an arrow marks the phase transition temperature T_c. Red dotted, green dashed and black solid lines represent least-squares fits of theoretical curves calculated within the α-model and for the nuclear Schottky effect, as indicated in a legend. For details of the fits, see the text. Inset: blowup of the lowest temperature part of the plot.

Another way to estimate the electron-phonon coupling constant λ_{el-ph} is by using the phenomenological relation $\lambda^b_{el-ph} = \gamma_n/\gamma_b - 1$ with two values of the Sommerfeld coefficient: the experimental one ($\gamma_n = 7.0\ \mathrm{mJK^{-2}mol^{-1}}$) given above and the calculated ($\gamma_b = 5.29\ \mathrm{mJK^{-2}mol^{-1}}$) from first principles value from our previous study [8]. In such a way, one gets an even lower value of $\lambda^*_{el-ph} = 0.32$.

The low-temperature dependence of the non-phononic (i.e. sum of the electronic and nuclear) specific heat $C_{el}(T) + C_{nuc}(T)$, obtained by subtraction of the lattice term βT^3 from the total specific heat $C_P(T)$, is shown in figure 3. From this plot we found that the normalized specific heat jump $\Delta C/(\gamma_n T_c)$ at the critical temperature T_c in single-crystalline $LuPd_2Si_2$ is equal to 1.31, which is noticeably lower than $(\Delta C/(\gamma_n T_c))_{BCS} = 1.43$ expected from the BCS theory of superconductivity. This difference can be explained in terms of the α-model [18, 19] and the relation:

$$\frac{\Delta C}{\gamma_n T_c} = \left(\frac{\Delta C}{\gamma_n T_c}\right)_{BCS}\left(\frac{\alpha}{\alpha_{BCS}}\right)^2, \quad (3)$$

with $\alpha_{BCS} = 1.764$ predicted by the BCS theory, which for $\Delta C/(\gamma_n T_c) = 1.31$ gives $\alpha = 1.688$. However, as can be seen in figure 3, the temperature dependence of the electronic specific heat simulated for the α-model (for details see [18, 19]) with $\alpha = 1.688$ (plotted as a red dotted line) describes well the experimental data only in the temperature range 0.3–0.6 K, while at lower temperatures a clear discrepancy between the theoretical and experimental curves is observed. In addition, below about 150 mK, a small increase of the specific heat with decreasing T is observed that cannot be accounted for by the α-model.

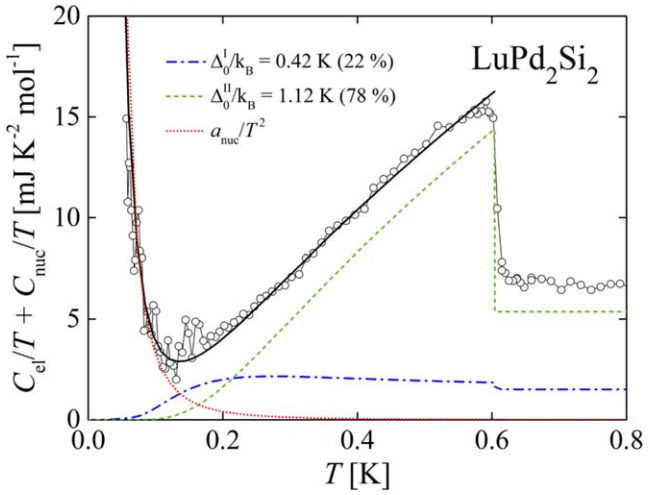

Figure 4. Low-temperature electronic specific heat of single-crystalline $LuPd_2Si_2$, plotted as C_{el}/T versus T, together with a fit of two-gap α-model of the superconductivity and nuclear Schottky contribution (black solid line). Dotted, dashed and dash-dotted curves show particular contributions to C_{el} as listed in the legend. For details see the text.

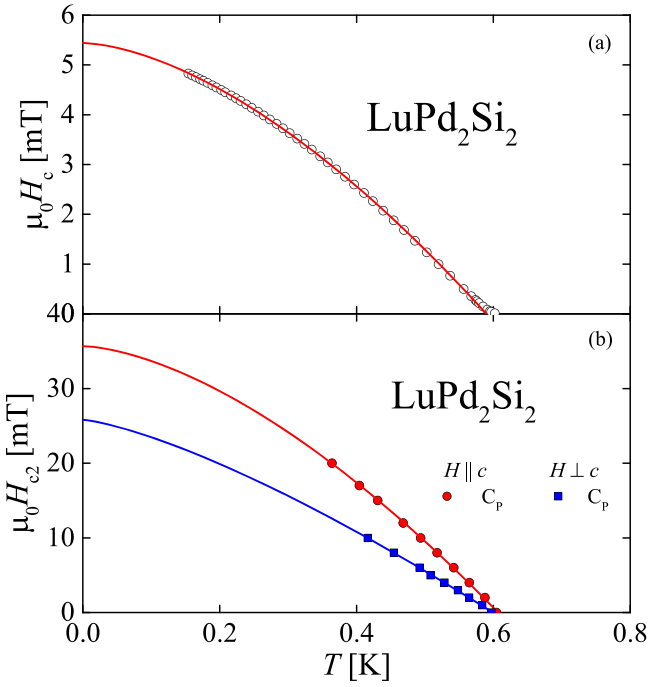

Figure 5. Temperature dependences of (a) thermodynamic critical field H_c and (b) upper critical field H_{c2} for two directions of applied magnetic field; solid lines are fits of equation (6) (panel (a)) and equation (8) (panel (b)) to the experimental data.

Some improvement of the fit (see the green dashed line in figure 3) can be achieved by taking into account the nuclear Schottky contribution to the specific heat, a_{nuc}/T^2, originating from nuclear magnetic moments. Least-squares fit of such a term to the experimental data (as an addition to the α-model) yielded $a_{nuc} = 3.3 \times 10^{-3}$ mJKmol^{-1}.

In order to achieve a satisfactory fit of the model to the experimental data throughout the entire temperature range of the superconducting state, we considered occurrence of two gaps in the energy spectrum of $LuPd_2Si_2$, as observed for filled skutterudites $LaRu_4As_{12}$ [20] and $LaOs_4As_{12}$ [21], in which very similar small excess of the specific heat was found. In this approach, the electronic specific heat of $LuPd_2Si_2$ was expressed as (see e.g. [22, 23]):

$$C_{el} = xC_{el}(\Delta_0^{I}) + (1 - x)C_{el}(\Delta_0^{II}), \tag{4}$$

where $C_{el}(\Delta_0^{I})$ and $C_{el}(\Delta_0^{II})$ are the electronic specific heat contributions corresponding to two different values of the superconducting energy gap (Δ_0^{I} and Δ_0^{II}, respectively), x is equal to γ_1/γ_n and $1-x = \gamma_2/\gamma_n$. Using a sum of the electronic specific heat described by equation (4) and previously determined a_{nuc}/T^2 we were able to describe satisfactorily the experimental $C_{el}(T)$ in the superconducting range with the parameters $\Delta_0^{I}/k_B = 0.42$ K, $\Delta_0^{II}/k_B = 1.12$ K and $x = 0.22$, which leads to $\gamma_1 = 1.54$ mJK^{-2}mol^{-1} and $\gamma_2 = 5.46$ mJK^{-2}mol^{-1} (see the black solid line in figure 3). In order to make it even more convincing, the experimental data are plotted in figure 4 as $C_{el}(T)/T + C_{nuc}(T)/T$ together with the successful fit and particular contributions, including the normal-state electronic specific heat.

From the experimental specific heat data collected in the superconducting state (in zero magnetic field), C_s, and in the normal state (in 25 mT), C_n, and using the thermodynamic equations (cf e.g. [24] and references therein):

$$-\frac{1}{2}V_{mol}H_c^2(T) = \Delta U(T) - T\Delta S(T), \tag{5a}$$

$$\Delta U(T) = \int_T^{T_c} [C_s(T') - C_n(T')]dT', \tag{5b}$$

$$\Delta S(T) = \int_T^{T_c} \frac{C_s(T') - C_n(T')}{T'}dT', \tag{5c}$$

one can derive for $LuPd_2Si_2$ the temperature dependence of the thermodynamic critical field $H_c(T)$ (figure 5(a)). Because of the low-temperature upturn in C_{el}, our calculations were limited to temperatures higher than 150 mK.

In order to determine the thermodynamic critical field at 0 K, $\mu_0 H_c(0)$, the commonly used power-law relation:

$$\mu_0 H_c(T) = \mu_0 H_c(0)\left[1 - \left(\frac{T}{T_c}\right)^n\right], \tag{6}$$

was fitted to the data plotted in figure 5(a). The least-squares fitting procedure yielded the parameters $\mu_0 H_c(0) = 5.4$ mT, $T_c = 0.60$ K and $n = 1.64$. A similar value of $\mu_0 H_c(0) = 5.3$ mT was obtained from the equation (cf e.g. [25]):

$$\mu_0 V_{mol} H_c^2 = \frac{3\gamma_n}{2\pi^2 k_B^2}\Delta_0^2, \tag{7}$$

using the experimentally determined parameters $\gamma_n = 7.0$ mJmol^{-1} K^{-2}, $V_{mol} = 49.6 \times 10^{-6}$ m^{3}mol^{-1} and $\Delta_0/k_B = 1.01$ K (corresponding to $\alpha = 1.688$).

Table 1. Basic characteristics of superconductivity in single-crystalline $LuPd_2Si_2$.

Parameter	Value	
	$H \parallel c$	$H \perp c$
T_c [K]	0.60	
γ_n [mJK^{-2}mol^{-1}]	7	
γ_b [mJK^{-2}mol^{-1}]	5.29 [8]	
β [mJK^{-4}mol^{-1}]	0.28	
Θ_D [K]	327	
λ_{el-ph}	0.41	
$N_b(E_F)$ [eV^{-1}f.u.$^{-1}$]	2.1	
λ^b_{el-ph}	0.32	
$\Delta C/(\gamma_n T_c)$	1.31	
α	1.688	
α^I	0.70	
Δ^I_0/k_B [K]	0.42	
γ_1 [mJK^{-2}mol^{-1}]	1.54	
α^{II}	1.85	
Δ^{II}_0/k_B [K]	1.12	
γ_2 [mJK^{-2}mol^{-1}]	5.46	
$\mu_0 H_c(0)$ [mT]	5.4	
n	1.64	
V_{mol} [m^{3}mol^{-1}]	49.6×10^{-6}	
Δ_0/k_B [K]	1.01	
$\mu_0 H_P$ [T]	1.1	
$\mu_0 H_{c2}(0)$ [mT]	35.6	25.8
m	1.60	1.34
$d(\mu_0 H_{c2}(T))/dT\|_{T_c}$ [mT/K]	-87.7	-64.1
$\mu_0 H^{orb}_{c2}$('clean') [mT]	38.5	28.1
$\mu_0 H^{orb}_{c2}$('dirty') [mT]	36.7	26.8
ξ_{GL} [nm]	96	113
λ_{GL} [nm]	447	382
κ	4.66	3.38

The $C_P(T)$ curves measured in various magnetic fields allowed us to derive the temperature dependences of the upper critical field $H_{c2}(T)$ for the two configurations of the magnetic field in relation to the crystallographic axes (figure 5(b)). The so-obtained curves can be well described by the power-law formula:

$$\mu_0 H_{c2}(T) = \mu_0 H_{c2}(0)\left[1 - \left(\frac{T}{T_c}\right)^m\right], \tag{8}$$

with the least-squares fitting parameters gathered in table 1.

Taking the initial slope of the $H_{c2}(T)$ experimental curves, defined as $d(\mu_0 H_{c2}(T))/dT|_{T_c}$ and equal to -87.7 mT/K ($H \parallel c$) and -64.1 mT/K ($H \perp c$), one can estimate the orbital limiting field $\mu_0 H^{orb}_{c2}$ using the formula:

$$\mu_0 H^{orb}_{c2} = -AT_c\left[\frac{d(\mu_0 H_{c2}(T))}{dT}\right]_{T_c}, \tag{9}$$

where A takes a value of 0.727 and 0.693 for the clean and dirty limits, respectively. The calculations yielded $\mu_0 H^{orb}_{c2} = 38.5$ mT for $H \parallel c$ and 28.1 mT for $H \perp c$ in the clean limit scenario and 36.7 mT for $H \parallel c$ and 26.8 mT for $H \perp c$ in the dirty limit one. It is worth noting that the obtained values of the limiting orbital field $\mu_0 H^{orb}_{c2}$ and the upper critical field $\mu_0 H_{c2}(T)$ in $LuPd_2Si_2$ are very similar. Moreover, they are distinctly smaller than the Pauli–Clogston–Chandrasekhar limiting field in this compound $\mu_0 H_P = 1.86\, T_c = 1.1$ T. This finding indicates that orbital pair breaking is the main factor responsible for destroying the superconducting state in $LuPd_2Si_2$. Interestingly, most of the known multi-band superconductors exhibit much larger values of the upper critical field.

From the values of $\mu_0 H_c(0)$ and $\mu_0 H_{c2}(0)$ one can determine the Ginzburg–Landau parameter κ. For $LuPd_2Si_2$ one gets $\kappa = 4.66$ and 3.38 for $H \parallel c$ and $H \perp c$, respectively, pointing to type-II superconductivity.

The coherence length ξ_{GL} can be estimated from the relationship:

$$\mu_0 H_{c2} = \frac{\Phi_0}{2\pi\xi^2_{GL}}, \tag{10}$$

where $\Phi_0 = h/2e = 2.0678 \times 10^{-15}$ Tm^2 is the magnetic flux quantum. In $LuPd_2Si_2$, ξ_{GL} takes the values of 96 nm and 113 nm for $H \parallel c$ and $H \perp c$, respectively. In turn, from the definition of the Ginzburg–Landau parameter:

$$\kappa = \lambda_{GL}(T)/\xi_{GL}(T), \tag{11}$$

one can estimate values of the penetration depth $\lambda_{GL} = 447$ nm for $H \parallel c$ and 382 nm for $H \perp c$. All the parameters characterizing the superconducting state in $LuPd_2Si_2$ are gathered in table 1.

4. Concluding remarks

Our heat capacity study on single-crystalline $LuPd_2Si_2$ corroborated the emergence of a superconducting state below 0.60 K. Detailed analysis of temperature and field variations of the specific heat revealed that the superconductivity in this compound is BCS-like, yet anisotropic and possibly of a two-gap character.

The lack of a convex shape of the $H_{c2}(T)$ curve near T_c in figure 5(b) is not an argument against the two-gap superconductivity in $LuPd_2Si_2$, although such a shape is observed in the best-known two-gap superconductors, e.g. MgB_2 [26], $NbSe_2$ [27], YNi_2B_2C and $LuNi_2B_2C$ [28]. First, the convex shape of the $H_{c2}(T)$ curve for most of the known two-gap superconductors is visible only for $T/T_c \approx 1$, thus—from the experimental point of view—it is easier to observe that feature in superconductors with higher critical temperature, with only a few exceptions (see e.g. [29, 30]). Second, for some two-gap superconductors this feature is not observed at all (see e.g. $Lu_2Fe_3Si_5$ [31]) or it is observed only for magnetic fields oriented in some particular direction (see e.g. $NbSe_2$ [32]). Third, the temperature dependence of the upper critical field is particularly sensitive to the strength of coupling between the two bands or the intensity of intraband impurity scattering [33, 34], making the observation of the convex shape of $H_{c2}(T)$ curve very difficult or impossible in some cases.

Fourth, the convex shape is usually more visible in $H_{c2}(T)$ curves derived from resistivity measurements. For instance, our recently reported results for YPd_2Ge_2 [11] and YPd_2Si_2 [12] have shown an upward curvature for $H_{c2}(T)$ dependencies obtained from the electrical resistivity $\rho(T, H)$ data and no such a feature in the respective curves derived from specific heat $C_P(T, H)$ and magnetization $M_{mol}(H)$ (even though both compounds have not been evidenced as multi-band superconductors so far). Moreover, $LuRu_4As_{12}$, showing very small excessive specific heat in comparison to the prediction of BCS theory for single gap superconductors, was recently established as a two-gap superconductor based on local magnetization studies [35]. All these features show that the two-gap superconductivity scenario is quite probable for $LuPd_2Si_2$.

Nevertheless, it should be noted that the anisotropic gap models (see e.g. [36]) might provide a comparably good description of the experimental data results, so it is often difficult to distinguish between them based only on the temperature dependencies of the specific heat and related quantities. Some premises for or against the two-gap scenario could be deduced from the field dependence of the Sommerfeld coefficient, however in the case of $LuPd_2Si_2$, any reliable analysis is very difficult due to the presence of the nuclear Schottky effect. Therefore, the question of two-gap superconductivity remains open—further investigations are needed to confirm or exclude the latter hypothesis.

Acknowledgments

This work was financially supported by the National Centre of Science (NCN, Poland) within a research grant no. 2014/13/B/ST3/04544.

ORCID iDs

G Chajewski https://orcid.org/0000-0001-7700-9685
P Wiśniewski https://orcid.org/0000-0002-6741-2793
D Gnida https://orcid.org/0000-0003-3813-6387
A P Pikul https://orcid.org/0000-0002-5998-0707
D Kaczorowski https://orcid.org/0000-0002-8513-7422

References

[1] Szytuła A and Leciejewicz J 1989 Magnetic properties of ternary intermetallic compounds of the RT_2X_2 type *Handbook on the Physics and Chemistry of Rare Earths* vol 12 (Amsterdam: Elsevier) pp 133–211
[2] Stewart G R 2011 *Rev. Mod. Phys.* **83** 1589–652
[3] Dai P 2015 *Rev. Mod. Phys.* **87** 855–96
[4] Pikul A P, Samsel-Czekała M, Chajewski G, Romanova T, Hackemer A, Gorzelniak R, Wiśniewski P and Kaczorowski D 2017 *J. Phys. Condens. Matter* **29** 195602
[5] Chajewski G, Samsel-Czekała M, Hackemer A, Wiśniewski P, Pikul A P and Kaczorowski D 2018 *Physica* B **536** 767–72
[6] Ciesielski K, Chajewski G, Samsel-Czekała M, Hackemer A, Pikul A P and Kaczorowski D 2017 *Solid State Commun.* **257** 32–5
[7] Ciesielski K, Chajewski G, Samsel-Czekała M, Hackemer A, Obstarczyk P, Pikul A and Kaczorowski D 2018 *Solid State Commun.* **280** 13–7
[8] Samsel-Czekała M, Chajewski G, Wiśniewski P, Romanova T, Hackemer A, Gorzelniak R, Pikul A P and Kaczorowski D 2018 *Physica* B **536** 816–20
[9] Domieracki K and Kaczorowski D 2016 *Acta Phys. Pol.* A **130** 593–6
[10] Domieracki K, Wiśniewski P, Wochowski K, Romanova T, Hackemer A, Gorzelniak R, Pikul A and Kaczorowski D 2018 *Physica* B **536** 734–7
[11] Chajewski G, Wiśniewski P, Hackemer A, Pikul A and Kaczorowski D 2018 *Physica* B **536** 761–6
[12] Chajewski G, Wiśniewski P, Gnida D, Pikul A P and Kaczorowski D 2019 *Cryst. Growth Des.* **19** 2557–63
[13] Palstra T T M, Lu G, Menovsky A A, Nieuwenhuys G J, Kes P H and Mydosh J A 1986 *Phys. Rev.* B **34** 4566–70
[14] Kaštil J, Diviš M, Vlášková K, Doležal P, Fikáček J, Prchal J, Míšek M, Kamarád J and Arnold Z 2018 *Intermetallics* **100** 171–4
[15] Rodríguez-Carvajal J 1993 *Physica* B **192** 55–69
[16] Hwang J S, Lin K J and Tien C 1997 *Rev. Sci. Instrum.* **68** 94–101
[17] McMillan W L 1968 *Phys. Rev.* **167** 331–44
[18] Padamsee H, Neighbor J E and Shiffman C A 1973 *J. Low Temp. Phys.* **12** 387–411
[19] Johnston D C 2013 *Supercond. Sci. Technol.* **26** 115011
[20] Bochenek L, Wawryk R, Henkie Z and Cichorek T 2012 *Phys. Rev.* B **86** 060511
[21] Juraszek J, Henkie Z and Cichorek T 2016 *Acta Phys. Pol.* A **130** 597–9
[22] Fisher R A, Li G, Lashley J C, Bouquet F, Phillips N E, Hinks D G, Jorgensen J D and Crabtree G W 2003 *Physica* C **385** 180–91
[23] Gofryk K, Sefat A S, Bauer E D, McGuire M A, Sales B C, Mandrus D, Thompson J D and Ronning F 2010 *New J. Phys.* **12** 023006
[24] Sahakyan M and Tran V H 2016 *J. Phys. Condens. Matter* **28** 205701
[25] Tran V H, Bukowski Z, Wiśniewski P, Tran L M and Zaleski A J 2013 *J. Phys. Condens. Matter* **25** 155701
[26] Müller K H, Fuchs G, Handstein A, Nenkov K, Narozhnyi V N and Eckert D 2001 *J. Alloys Compd.* **322** L10–3
[27] Toyota N, Nakatsuji H, Noto K, Hoshi A, Kobayashi N, Muto Y and Onodera Y 1976 *J. Low Temp. Phys.* **25** 485–99
[28] Shulga S V, Drechsler S L, Fuchs G, Müller K H, Winzer K, Heinecke M and Krug K 1998 *Phys. Rev. Lett.* **80** 1730–3
[29] Jaroszynski J *et al* 2008 *Phys. Rev.* B **78** 064511
[30] Kano M, Kohama Y, Graf D, Balakirev F, Sefat A S, Mcguire M A, Sales B C, Mandrus D and Tozer S W 2009 *J. Phys. Soc. Japan* **78** 084719
[31] Nakajima Y, Nakagawa T, Tamegai T and Harima H 2008 *Phys. Rev. Lett.* **100** 157001
[32] Sanchez D, Junod A, Muller J, Berger H and Lévy F 1995 *Physica* B **204** 167–75
[33] Suhl H, Matthias B T and Walker L R 1959 *Phys. Rev. Lett.* **3** 552–4
[34] Mansor M and Carbotte J P 2005 *Phys. Rev.* B **72** 024538
[35] Juraszek J, Wawryk R, Henkie Z, Konczykowski M and Cichorek T 2020 *Phys. Rev. Lett.* **124** 027001
[36] Zehetmayer M 2013 *Supercond. Sci. Technol.* **26** 043001